THE JOURNAL OF BIOLOGICAL CHEMISTRY VOL. 287, NO. 36, pp. 30346–30357, August 31, 2012

Thioredoxin Reductase Linked to Cytoskeleton by Focal Adhesion Kinase Reverses Actin *S*-Nitrosylation and Restores Neutrophil β_2 Integrin Function*

Received for publication, February 23, 2012, and in revised form, June 28, 2012 Published, JBC Papers in Press, July 9, 2012, DOI 10.1074/jbc.M112.355875

Stephen R. Thom[‡§1], **Veena M. Bhopale**[‡], **Tatyana N. Milovanova**[‡], **Ming Yang**[‡], **and Marina Bogush**[‡]

From the [‡]*Institute for Environmental Medicine and the* [§]*Department of Emergency Medicine, University of Pennsylvania Medical Center, Philadelphia, Pennsylvania 19104*

Background: Hyperbaric oxygen inhibits neutrophil β_2 integrin adherence, but mechanisms for reversal are unclear.
Results: Thioredoxin reductase reverses cytoskeletal changes due to hyperoxia when kept in proximity to short filamentous actin by focal adhesion kinase.
Conclusion: Cell activation causes sequential protein associations with actin to restore integrin adherence function.
Significance: Intermittent hyperoxia can have benefits, and results show why it does not concomitantly inhibit neutrophil antibacterial functions.

The investigation goal was to identify mechanisms for reversal of actin *S*-nitrosylation in neutrophils after exposure to high oxygen partial pressures. Prior work has shown that hyperoxia causes *S*-nitrosylated actin (SNO-actin) formation, which mediates β_2 integrin dysfunction, and these changes can be reversed by formylmethionylleucylphenylalanine or 8-bromo-cyclic GMP. Herein we show that thioredoxin reductase (TrxR) is responsible for actin denitrosylation. Approximately 80% of cellular TrxR is localized to the cytosol, divided between the G-actin and short filamentous actin (sF-actin) fractions based on Triton solubility of cell lysates. TrxR linkage to sF-actin requires focal adhesion kinase (FAK) based on immunoprecipitation studies. *S*-Nitrosylation accelerates actin filament turnover (by mechanisms described previously (Thom, S. R., Bhopale, V. M., Yang, M., Bogush, M., Huang, S., and Milovanova, T. (2011) Neutrophil β_2 integrin inhibition by enhanced interactions of vasodilator stimulated phosphoprotein with *S*-nitrosylated actin. *J. Biol. Chem.* 286, 32854–32865), which causes FAK to disassociate from sF-actin. TrxR subsequently dissociates from FAK, and the physical separation from actin impedes denitrosylation. If SNO-actin is photochemically reduced with UV light or if actin filament turnover is impeded by incubations with cytochalasin D, latrunculin B, 8-bromo-cGMP, or formylmethionylleucylphenylalanine, FAK and TrxR reassociate with sF-actin and cause SNO-actin removal. FAK-TrxR association can also be demonstrated using isolated enzymes in *ex vivo* preparations. Uniquely, the FAK kinase domain is the site of TrxR linkage. We conclude that through its scaffold function, FAK influences TrxR activity and actin *S*-nitrosylation.

Neutrophil β_2 integrin adhesion molecules participate in regulating neutrophil activation and endothelial adhesion (1). When animals or humans are exposed to hyperbaric oxygen (HBO_2)[2] at 2.8–3.0 atmospheres absolute (ATA), β_2 integrins on circulating neutrophils are temporarily inhibited (2–6). This action is linked to improved outcomes from inflammatory and reperfusion injuries in a number of animal models and clinical trials (2, 6–19). Importantly, hyperoxia does not appear to cause immunocompromise, contrary to some other integrin-blocking interventions (2, 3, 20–25). Understanding mechanisms for this combination of favorable effects was the basis for this line of investigation.

Hyperoxia increases production of reactive species derived from nitric-oxide synthase and myeloperoxidase, which cause *S*-nitrosylation of β-actin (26). HBO_2-exposed cells exhibit greater actin filament (F-actin) turnover, which inhibits β_2 integrin clustering and thus β_2 integrin adhesion (26). Vasodilator-stimulated protein (VASP) has high affinity for *S*-nitrosylated short filamentous actin (sF-actin) (27). VASP bundles Rac 1, Rac 2, and cyclic AMP-dependent and cyclic GMP-dependent protein kinases in close proximity to sF-actin, and subsequent Rac activation increases actin free barbed end formation. fMLP and 8-bromo-cyclic GMP (8-Br-cGMP) reverse these events because they activate, respectively, either cyclic AMP-dependent or cyclic GMP-dependent protein kinase outside of the sF-actin pool, which phosphorylates VASP. This reduces VASP affinity for sF-actin. Decreased VASP binding to actin resolves the elevated Rac activity and abrogates the augmented polymerization normally observed with *S*-nitrosylated actin. Thus, fMLP and 8-Br-cGMP can restore normal β_2 integrin function. Demonstrating restoration of function with the bacterial product fMLP provides a partial explanation for why HBO_2 does not cause immunocompromise despite improving

* This work was supported by a grant from the Office of Naval Research.
[1] To whom correspondence should be addressed: Institute for Environmental, Medicine, University of Pennsylvania, 1 John Morgan Bldg., 3620 Hamilton Walk, Philadelphia, PA 19104-6068. Tel.: 215-898-9095; Fax: 215-573-7037; E-mail: sthom@mail.med.upenn.edu.

[2] The abbreviations used are: HBO_2, hyperbaric oxygen; fMLP, formylmethionylleucylphenylalanine; SNO-actin, *S*-nitrosylated actin; ATA, atmospheres absolute; VASP, vasodilator-stimulated protein; F-actin, filamentous actin; sF-actin, short filamentous actin; 8-Br-cGMP, 8-bromo-cyclic GMP; TrxR, thioredoxin reductase(s); FAK, focal adhesion kinase; SNAP, *S*-nitroso-*N*-acetyl-DL-penicillamine; NS, not significant; FBE, free barbed end; ANOVA, analysis of variance.

outcomes from some inflammatory and reperfusion injuries (28, 29).

HBO_2-exposed neutrophils no longer exhibit elevated content of *S*-nitrosylated actin (SNO-actin) after incubation with fMLP or 8-Br-cGMP (26). Identifying how actin *S*-nitrosylation is reversed was the goal for the current research effort. Denitrosylation of cytosolic proteins is performed by NADPH-dependent thioredoxin reductases (TrxR) and NADH-dependent *S*-nitrosoglutathione reductase. A third enzyme, NADH-dependent lipoamide dehydrogenase, is a part of the α-keto acid dehydrogenase complex in mitochondria, where it denitrosylates low molecular weight *S*-nitrosothiols; only a small fraction of the enzyme is found in cytosol (30, 31). There are three TrxR isoenzymes. TrxR1 is predominantly cytosolic, most TrxR2 is found in mitochondria, and the third isoenzyme contains an additional mono-thiol glutaredoxin domain and is mainly expressed in early spermatids in the testis (32–35). TrxR and *S*-nitrosoglutathione reductase cooperate in a complex, conjoined fashion to regulate cell denitrosylation (36, 37), and there is also cross-talk between the glutathione and thioredoxin systems. TrxR, lipoamide dehydrogenase, and glutathione reductase can reduce the disulfide lipoic acid (5-[1,2]-dithiolan-3-yl-pentanoic acid) to dihydrolipoic acid, which will denitrosylate proteins (30).

Bidirectional integrin-actin communications are required for proper cell functioning, and coordination of many of these activities involves focal adhesion kinase (FAK) (38). Interactions among many proteins impinge on FAK to control β_2 integrin-focal contact turnover (39–41). FAK consists of an N-terminal FERM (band four point one radixin, ezrin, moesin) homology domain, followed by a tyrosine kinase domain and a C-terminal focal adhesion targeting (FAT) domain. The exact function of FAK in neutrophils has not been clearly defined, but in most cell types, FAK is predominantly a scaffolding protein. It appears to modulate integrin-cytoskeletal associations, and it may enhance actin polymerization (42–44). Links to the actin cytoskeleton and regulation of cell motility, proliferation, and oncogenic transformation involve adaptor proteins, such as paxillin or talin, that bind integrin cytoplasmic tails and the C-terminal FAT region of FAK (45–47). The N-terminal FERM domain coordinates FAK activation by several growth factors (48, 49). A direct interaction between FAK and integrins has not been clearly established, although *in vitro* the N-terminal domain binds to sequences in the cytoplasmic tail of β integrin subunits (47).

The purpose of this investigation was to elucidate the mechanism for SNO-actin removal in cells exposed to fMLP or 8-Br-cGMP. In the course of these studies, a central role for TrxR was identified. As work progressed, it became clear that FAK played a role in modulating TrxR intracellular localization and activity.

EXPERIMENTAL PROCEDURES

Materials—Chemicals were purchased from Sigma-Aldrich unless otherwise noted. *N*-[6-(biotinamido)hexyl]-3′-(2′-pyridyldithio)propionamide and streptavidin-agarose were purchased from Prozyme (Hayward, CA). HisPur™ cobalt resin was purchased from Thermo Scientific/Pierce. PF 573228 (3,4-dihydro-6-[[4-[[[3-(methylsulfonyl)phenyl]methyl]amino]-5-(trifluoromethyl)-2-pyrimidinyl]amino]-2(1*H*)-quinolinone) was purchased from Tocris/R&D Systems (Minneapolis, MN). Ultrafree-MC filters, PVDF Immobilon-FL, and ZipTipC_{18}P10 were from Millipore Corp. Antibodies were purchased from the following vendors: anti-biotin and anti-actin (Sigma), anti-FAK (BD Biosciences), and anti-TrxR1 (Santa Cruz Biotechnology, Inc., Santa Cruz, CA). The following small inhibitory RNA (siRNA) sequences were purchased from Santa Cruz Biotechnology, Inc.: a control, scrambled sequence siRNA that will not cause specific degradation of any known cellular mRNA (UUCUCCGAACGUGUCACGU); TrxR1 siRNA, a mixture of three sequences identified as strand A (CUUGGCUAAUCUACUUGAA), strand B (GGAAGCUGUUCAUAACGUA), and strand C (GAAGCUGUUCAUAACGUAA); FAK siRNA, a mixture of three sequences, strand A (GCAUCCUGAAAUUCUUUGA), strand B (CCAGUACUCAAACAGUGAA), and strand C (CGACCAGGGAUUAUGAGAU; *S*-nitrosoglutathione reductase siRNA, a pool of three different siRNA duplexes, strand A (sense, CAUGAAGUUCGGAUUAAGAtt; antisense, UCUUAAUCCGAACUUCAUGtt), strand B (sense, GCAUAAUCGAGACUGUAAUtt; antisense, AUUACAGUCUCGAUUAUGCtt), and strand C (sense, CAUCCACAUGGGUUUAGAAtt; antisense, UUCUAAACCCAUGUGGAUGtt); and glutathione reductase siRNA, also a pool of three different siRNA duplexes, strand A (sense, CCAUGAUUCCAGAUGUUGAtt; antisense, UCAACAUCUGGAAUCAUGGtt), strand B (sense, CGAAGCUGUUCAUAAGUAUtt; antisense, AUACUUAUGAACAGCUUCGtt), and strand C (sense, GUACAUGACAUACACUCAAtt; antisense, UUGAGUGUAUGUCAUGUACtt).

Animals—Mice (*Mus musculus*) were purchased (Jackson Laboratories, Bar Harbor, ME), fed a standard rodent diet and water *ad libitum*, and housed in the animal facility of the University of Pennsylvania. After anesthesia (intraperitoneal administration of ketamine (100 mg/kg) and xylazine (10 mg/kg)), skin was prepared by swabbing with Betadine, and blood was obtained into heparinized syringes by aortic puncture.

Isolation of Neutrophils and Exposure to Various Agents—Mice were anesthetized, and neutrophils were isolated from heparinized blood as described previously (26). A concentration of 5×10^5 neutrophils/ml of PBS plus 5.5 mM glucose was exposed to either air or 2.0 ATA O_2 for 45 min (we have shown that *ex vivo* exposures to 1 or 2 ATA O_2 are equivalent to *in vivo* exposures to 2.8 ATA (26)). After air/O_2 exposures but prior to specific studies, cell suspensions were incubated for 10 min with a chemical agonist or inhibitor or exposed for 5 min to UV light from a 200-watt mercury vapor lamp. Where indicated, after air/O_2 exposures but before studies, cells were incubated for 20 h at room temperature with siRNA following the manufacturer's instructions using control, scrambled sequence siRNA that will not lead to specific degradation of any known cellular mRNA or siRNA specific for mouse TrxR1, glutathione reductase, *S*-nitrosoglutathione reductase, or FAK. Pilot studies demonstrated that concentrations of 0.08 nM achieved maximum decreases in protein levels.

Fibrinogen-coated Plate Adherence—Preparation and use of fibrinogen-coated plates to measure β_2 integrin-specific neutrophil adherence in calcein AM-loaded cells was as described

previously (26). Suspensions of 25,000 cells in 100 μl of PBS were added to plate wells containing either PBS or solutions, so that once added, cells would be exposed to 100 μM 8-Br-cGMP or 100 nM fMLP. At the end of the 10-min incubation, wells were washed, and adherence was calculated as described previously (26).

Cell Extract Preparation and Biotin Switch Assay—Isolated neutrophils previously exposed to air (control) or HBO_2 were suspended in 2 ml of HEN buffer (250 mM Hepes, pH 7.7, 1 mM EDTA, 0.1 mM neocuproine), sonicated on ice for 30 s, and then passed through a 28-gauge needle five times. Lysates were centrifuged at 2000 × *g* for 10 min, supernatant was recovered, and samples were made 0.4% CHAPS using the 10% stock solution. The biotin switch assay was carried out following published methods, including 20 nM $CuCl_2$, as recommended by others (26, 50). It should be noted that biotinylation impedes antibody recognition of actin on Western blots so that small portions of cell preparation are not subjected to biotin switch procedures in order to quantify the total amount of actin present in each cell sample.

Confocal Microscopy—Isolated neutrophils exposed to air or HBO_2 were placed on slides coated with fibrinogen following published methods (26). Cells were permeabilized by incubation for 1 h at room temperature with PBS containing 0.1% (v/v) Triton X-100 and 5% (v/v) fetal bovine serum. Cells were then incubated overnight with 1:200 dilutions of Alexa 488-conjugated phalloidin plus primary antibodies to either FAK or TrxR. The next morning slides were rinsed three times with PBS and counterstained with a 1:500 dilution of APC and RPE-conjugated secondary antibodies. Images of neutrophils were acquired using a Zeiss Meta510 confocal microscope equipped with a Plan-Apochromat ×63/1.4 numerical aperture oil objective. Fluorophore excitation was provided by 488- and 543-nm laser lines, and resulting fluorescence was separated using 500–530- and 560–615-nm band pass filters.

Cytoskeletal Protein Analysis Based on Triton Solubility—Neutrophils were processed following our published protocol (26). In brief, cells were suspended in 300 μl of cytoskeleton stabilization buffer (CSK; 25 mM HEPES, pH 6.9, 0.2% Triton X-100, 1 M glycerol, 1 mM EGTA, 1 mM PMSF, 1 mM $MgCl_2$), incubated for 10 min at room temperature, and then centrifuged at 15,000 × *g* for 5 min to obtain the Triton-insoluble pellets. Supernatant was centrifuged at 366,000 × *g* for 5 min, and the supernatant Triton-soluble G-actin was set aside. The Triton-soluble F-actin pellet was resuspended in CSK buffer and centrifuged at 300 × *g* for 10 min to remove debris. Where indicated, both the Triton-soluble and Triton-insoluble proteins were subjected to electrophoresis in SDS-4–15% gradient polyacrylamide gels and Western blotting (26) or subjected to immunoprecipitation. Triton-insoluble proteins were dissolved with SDS buffer heated to 95 °C and then subjected to electrophoresis followed by Western blotting.

TrxR Activity—Cell lysates containing 0.75 μg of cell protein per 20 μl of CSK buffer were analyzed following the method described by Hill *et al.* (51) with TrxR activity determined as the difference between the time-dependent increase in 412-nm light absorbance caused by 5 mM 5,5′-dithiobis(2-nitrobenzoic acid) in suspensions prepared without *versus* with 1 μM auranofin (triethylphosphine gold thioglucose tetra-acetate), a TrxR inhibitor. 5,5′-Dithiobis(2-nitrobenzoic acid) reduction was calculated using an extinction coefficient of 13.6×10^3 mol^{-1} cm^{-1} and expressed as units of activity defined as μmol of TNB/mg of protein/min.

TrxR Protection of Actin from S-Nitrosylation—Samples of sF-actin from neutrophils incubated for 20 h with control siRNA or siRNA to TrxR or FAK were suspended in HEN buffer and then divided into two equal samples for incubation without or with 20 μM auranofin plus 200 μM *S*-nitroso-*N*-acetyl-DL-penicillamine (SNAP) for 1 h at room temperature in the dark. Samples were then made 0.4% CHAPS using the 10% stock solution and subjected to the biotin switch assay.

Immunoprecipitation of Protein Complexes—Suspensions of G-actin and short F-actin containing 250 μg of protein were precleared and then incubated with antibodies (5 μg) on a shaker overnight at 4 °C, and then 30 μl of 20% (w/v) protein G-Sepharose (preblocked with 2% BSA) was added and incubated for 1.5 h at 4 °C. Samples were washed twice in CSK buffer, pelleted, resuspended in 20 μl of heated SDS buffer (62.5 mM Tris-HCl, 2% SDS, 10% glycerol, 20% β-mercaptoethanol), incubated at 95 °C for 15–20 min, and then subjected to electrophoresis and analyzed by Western blotting (26).

Protein and Peptide Analysis—Mass spectrometry (MS) and protein sequencing of immunoprecipitates were done by the Proteomics Core Facility of the Genomics Institute and the Abramson Cancer Center, University of Pennsylvania. Protein bands were cut from nitrocellulose paper, trypsin-digested, and analyzed with a nano-LC/nanospray/LTQ mass spectrometer following published methods (52). The raw data from MS/MS spectra were acquired with Sequest and analyzed with Scaffold 3.3. The cut-off value for peptide *p* values was <95%; for proteins, it was <99.0%.

Ex Vivo FAK-TrxR Interaction—Solutions of rat liver TrxR1 (1 μg/100 μl) and His-tagged human kinase domain of FAK (4 μg/100 μl) were prepared in equilibration buffer (50 mM sodium phosphate, 300 mM sodium chloride, 10 mM imidazole, pH 7.4). Prior to use, HisPur™ cobalt resin was washed twice with SDS buffer and then with elution buffer (50 mM sodium phosphate, 300 mM sodium chloride, 150 mM imidazole, pH 7.4) followed by four washes with PBS and prepared for use by suspension in incubation buffer.

Protein interactions were assessed by incubating TrxR solution (10 μl) with His-FAK solution (50 μl) for 1 h at room temperature with constant shaking. The mixture was then combined with 100 μl of cobalt resin followed by centrifugation at 700 × *g* for 2 min. Protein was eluted from the resin by incubation with elution buffer for 1 h at room temperature and then centrifuged for 2 min at 700 × *g*. The supernatant was combined with 2× SDS buffer for electrophoresis in SDS-4–15% gradient polyacrylamide gels followed by Western blotting (26). Blots were probed for TrxR and FAK.

The effect of FAK on TrxR activity was evaluated following the assay as described above. Before adding enzymes to buffer and 5,5′-dithiobis(2-nitrobenzoic acid), however, solutions of 11 μl of incubation buffer containing 0.1 μg of TrxR, 0.1 μg of TrxR plus 0.06 μg of His-FAK, or TrxR, FAK, and 5 μM PF

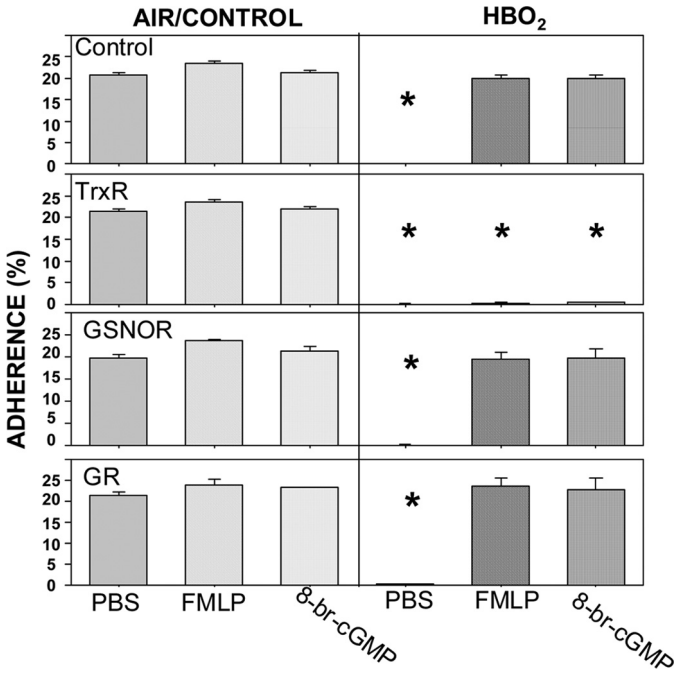

FIGURE 1. **β_2 integrin-specific neutrophil adherence.** Data show the fraction of neutrophils in a suspension that became adherent after incubation on fibrinogen-coated plates. Adherence was measured using neutrophils exposed to air (control) or 2.0 ATA O_2 for 45 min and then incubated for 20 h with control siRNA or siRNA to TrxR1, glutathione reductase, or *S*-nitrosoglutathione reductase. The next day, suspensions were loaded with calcein AM, divided, and placed in wells containing just PBS or PBS plus agonists to achieve a final concentration of 100 μM 8-Br-cGMP or 100 nM fMLP as described under "Experimental Procedures." The percentage adherence was calculated and compared against identical samples incubated with blocking antibodies to establish β_2 integrin-specific adherence. Data are mean ± S.E. (*error bars*); $n = 10$ separate studies using neutrophils from different animals; *, $p < 0.05$ *versus* control siRNA air-exposed cells incubated with just PBS.

573228 were incubated for 10 min at room temperature. Results were expressed as units of TrxR activity.

Statistical Analysis—Results are expressed as the mean ± S.E. for three or more independent experiments. To compare data, analysis of variance (ANOVA) (and, when appropriate, two-way ANOVA) was assessed using SigmaStat (Jandel Scientific, San Jose, CA) and Newman-Keuls post hoc test. The level of statistical significance was defined as $p < 0.05$.

RESULTS

Neutrophil β_2 Integrin-dependent Adherence—The inhibitory effect of HBO_2 on neutrophil β_2 integrin adherence and restoration of function after cells were incubated with fMLP or 8-Br-cGMP is shown in the *top panels* of Fig. 1. These studies were performed with normal cells exposed only to air (control) or hyperoxia for 45 min and then incubated overnight with control siRNA that does not cause specific degradation of any known cellular mRNA. The results are consistent with previous reports (26, 27). The *second series* of *panels* show that fMLP or 8-Br-cGMP did not restore adherence function if HBO_2-exposed cells had been incubated with siRNA to TrxR1. No abrogation of the fMLP or 8-Br-cGMP effects occurred, however, if cells were incubated with siRNA to *S*-nitrosoglutathione reductase or glutathione reductase (*third* and *fourth panel sets*), although enzyme depletion was comparable with that caused by TrxR1 siRNA (Table 1). We also found that incubation with

TABLE 1

Reduction in specified protein in neutrophils incubated with siRNA

Neutrophils incubated for 20 h with particular siRNA species were compared against cell samples incubated with control, scrambled sequence siRNA that will not lead to specific degradation of any known cellular mRNA. At the end of incubations, cells were lysed and subjected to Western blotting, and band density for specified proteins was normalized to the β-actin band on the same blot. Data show the reduction in protein band density/actin band density for cells incubated with siRNA against TrxR1, NADH-dependent *S*-nitrosoglutathione reductase (GSNOR), glutathione reductase (GR), or FAK relative to the ratio in cells incubated with control siRNA. Data are mean ± S.E. ($n = 4$–13) independent samples; values are not significantly different (ANOVA).

Protein	TrxR1	GSNOR	GR	FAK
Reduction (%)	69.8 ± 6.1	79.1 ± 11.4	55.5 ± 8.4	52.5 ± 5.3

the TrxR inhibitors 1-chloro-2,4-dinitrobenzene or auranofin had the same effect as siRNA to TrxR1 (Table 2). We conclude that TrxR1 is necessary for reversing HBO_2-mediated inhibition of neutrophil adherence.

As mentioned in the Introduction, lipoic acid will denitrosylate proteins, and several enzymes can reduce it to maintain its antioxidant function. In four replicate trials, after HBO_2-exposed neutrophils were incubated with TrxR1 siRNA and then with 1 mM lipoic acid, adherence was 18.2 ± 1.6%, and air-exposed cells treated similarly exhibited 19.5 ± 1.0% adherence (no significant difference; NS). Therefore, alternative antioxidant pathways remain intact despite TrxR1 depletion. All control experiments in this series resulted in similar degrees of neutrophil adherence. For example, HBO_2-exposed cells incubated with control siRNA and then with 1 mM lipoic acid while on fibrinogen-coated plates exhibited β_2 integrin-specific adherence of 19.2 ± 0.6%, and air-exposed, control neutrophils treated similarly exhibited adherence of 20.2 ± 0.4% (NS).

Interest in the role FAK may play in fMLP- and 8-Br-cGMP-mediated reversal of HBO_2-induced β_2 integrin inhibition was prompted by immunoprecipitation and imaging studies described below. Adherence after neutrophils were depleted of FAK by siRNA treatment is shown in Table 2. This manipulation abrogated fMLP and 8-Br-cGMP reversal, and a similar pattern was observed using PF 573228, a small chemical inhibitor of FAK kinase activity that interacts at the ATP-binding site (53).

Actin S-Nitrosylation in HBO_2-exposed Cells—Prior work has demonstrated that SNO-actin formation is the proximal event leading to HBO_2-mediated inhibition of neutrophil β_2 integrin adherence, and elevation of SNO-actin is not observed after HBO_2-exposed cells are incubated with fMLP or 8-Br-cGMP (26, 27). Results described above suggested that TrxR may be necessary for actin denitrosylation in cells incubated with fMLP or 8-Br-cGMP. *S*-Nitrosylation of neutrophil proteins was surveyed by the biotin switch assay, which covalently adds a disulfide-linked biotin to the labile *S*-nitrosylation sites on proteins. Western blots were probed with anti-biotin antibodies, and, in keeping with previous work (26), a 42 kDa band was reliably visualized (Fig. 2). On occasion, a faint band at ~34 kDa was identified. Bands cut from nitrocellulose paper and subjected to amino acid sequencing identified these proteins as actin and a partially degraded actin fraction, as was reported previously (26). For serial studies, the magnitude of biotin was normalized to actin loaded onto the gels. As described under "Experimental Procedures," this required Western blotting

TABLE 2

β_2 integrin-specific neutrophil adherence (%); inhibitor effects

Neutrophil suspensions were exposed to air (control) or 2.0 ATA O_2 for 45 min containing just PBS or containing PBS with 50 μM 1-chloro-2,4-dinitrobenzene, or 1 μM auranofin, and then adherence to fibrinogen-coated plates was measured as described under "Experimental Procedures" and in the legend to Fig. 1. Alternatively, neutrophils were first exposed to air or HBO_2 and then incubated for 20 h with siRNA to FAK before the adherence assay was performed, or they were incubated with 10 μM PF 573228 (FAK inhibitor) along with PBS, fMLP, or 8-Br-cGMP in the adherence assay. Data are mean ± S.E. (n = 3–8 separate studies using neutrophils from different animals).

Agent	Exposure	PBS	fMLP	8-Br-cGMP
		%	%	%
PBS	Air	24.3 ± 1.7	23.3 ± 1.6	23.2 ± 1.6
	HBO_2	0.2 ± 0.1[a]	23.6 ± 1.8	22.4 ± 1.5
PBS + DNCB	Air	25.2 ± 1.8	25.6 ± 1.4	25.2 ± 2.1
	HBO2	0.4 ± 0.3[a]	0.3 ± 0.8[a]	0.8 ± 0.7[a]
PBS + Auranofin	Air	21.2 ± 0.98	19.9 ± 1.3	20.2 ± 1.3
	HBO2	0.8 ± 0.9[a]	0.8 ± 0.9[a]	0.5 ± 0.4[a]
FAK siRNA	Air	20.6 ± 0.5	24.0 ± 0.6	21.4 ± 0.7
	HBO2	0.1 ± 0.1[a]	0.4 ± 0.2[a]	0.3 ± 0.1[a]
PF 573228	Air	20.6 ± 0.5	23.2 ± 0.3	20.3 ± 0.7
	HBO2	0.4 ± 0.2[a]	2.0 ± 0.3[a]	1.8 ± 0.3[a]

[a] $p < 0.05$ *versus* air-exposed cells incubated with just PBS.

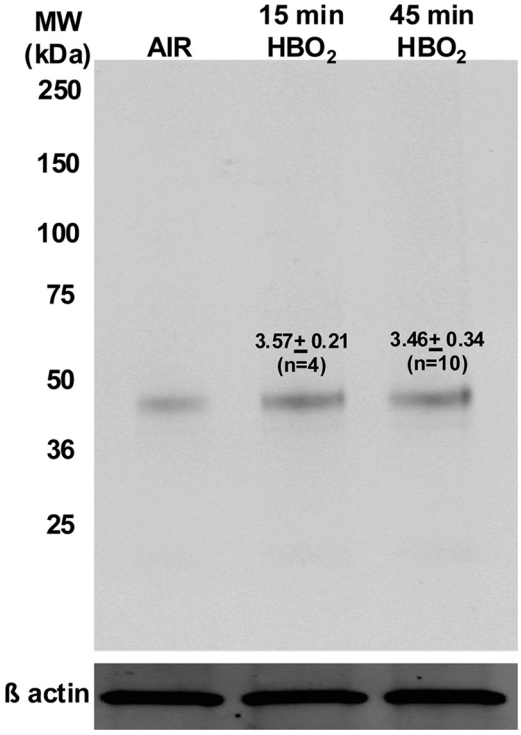

FIGURE 2. ***S*-Nitrosylated β-actin in neutrophil lysates.** Neutrophil suspensions were exposed to air (control) or to 2.0 ATA O_2 for 15 or 45 min, centrifuged, resuspended in HEN buffer, and processed for a biotin switch assay as described under "Experimental Procedures." The blots show a representative experiment; *numbers* shown on the image represent the -fold increase in SNO-actin band densities relative to control (air only) neutrophil lysates run on the same blots. Values are mean ± S.E. (*error bars*) for 4–10 independent trials (no significant difference).

using a separate sample from the cell lysate because the biotinylation procedure obscures protein recognition by anti-actin antibodies. As with previous studies, if the biotin switch analysis was performed on cell lysates treated with *N*-[6-(biotinamido)hexyl]-3′-(2′-pyridyldithio)propionamide or with ascorbate (but not both), with 1 mM $HgCl_2$, or if cells were exposed to UV light prior to cell lysis and biotin switch, the bands were not visualized (data not shown).

Fig. 3 shows results for cells incubated with either control siRNA or siRNA to TrxR1 and then exposed to PBS or PBS plus 8-Br-cGMP or fMLP. SNO-actin was over 3-fold elevated in HBO_2-exposed cells incubated with control siRNA, and this was reversed by exposure to 8-Br-cGMP and fMLP, consistent with previous reports (26, 27). If cells were incubated with siRNA to TrxR1, however, SNO-actin in HBO_2-exposed cells was not decreased by 8-Br-cGMP or fMLP.

These results led us to question whether the SNO-actin content of neutrophils might be impacted if F-actin turnover was inhibited. The basis for this idea was that SNO-actin causes a higher rate of filamentous actin turnover, and 8-Br-cGMP or fMLP abrogates this process (27). When HBO_2-exposed cells were incubated with cytochalasin D, the 3-fold elevation of SNO-actin (as shown in Figs. 2 and 3) no longer was observed, and the SNO-actin/total actin ratio was only 1.10 ± 0.06-fold different from control (n = 5, NS). Incubating control cells with cytochalasin D also did not alter biotinylation as compared with that in unmanipulated air-exposed cells; the ratio for SNO-actin/total actin was 1.04 ± 0.12 (n = 5, NS).

TrxR Cell Content and Activity—We next compared TrxR content and activity between control and HBO_2-exposed cells. Western analysis involving equal protein loading on gels demonstrated no difference in the TrxR content in whole cell lysates (Fig. 4). Similarly, when cell lysates were fractionated based on Triton solubility, the majority of TrxR appeared in the Triton-soluble short filamentous actin fraction. In these analyses, a second band with slightly greater molecular weight often was recognized by TrxR antibodies, but in whole cell lysates, a band with slightly lower molecular weight was seen on occasion. In the air-exposed, control cells, only 17.5 ± 8.5% (n = 8) of TrxR was in the Triton-insoluble fraction, and in HBO_2-exposed cells, there was 7.3 ± 2.5% (NS) in the Triton-insoluble fraction.

Surprisingly, although TrxR content was not significantly altered in HBO_2-exposed cells, TrxR activity in the cytosol was increased (Table 3). Moreover, the elevated activity was not found if HBO_2-exposed cells were incubated with fMLP or 8-Br-cGMP, cytochalasin D, or latrunculin B or if exposed to UV light to reverse actin *S*-nitrosylation after HBO_2 (Table 3).

In previous studies, we have reported that in HBO_2-exposed cells, the proportion of β-actin in the cytosolic short F-actin fraction was increased, and G-actin was decreased (26, 27). This was verified in the current study, where G-actin represented 32 ± 3% (n = 8) of total cell actin in air-exposed control cells and 24 ± 4% (n = 8, $p < 0.05$) in HBO_2-exposed cells, and short-F actin comprised 26 ± 4% in air-exposed control cells and 43 ± 6% ($p < 0.05$) in HBO_2-exposed cells. There was no significant difference in Triton-insoluble F-actin (42 ± 5% in air-exposed control cells and 33 ± 5% in HBO_2-exposed cells). Therefore, we also assess TrxR activity in actin fractions separated by Triton solubility. Elevated TrxR activity was present in the G-actin and sF-actin fractions of HBO_2-exposed cells (Table 3).

TrxR Immunoprecipitation and MS Identification—Given that TrxR activity was increased rather than being decreased in HBO_2-exposed cells, we considered that failure of TrxR to denitrosylate actin and restore adherence function with fMLP or 8-Br-cGMP incubation may occur due to alterations in TrxR association with actin. Initial studies were conducted with neu-

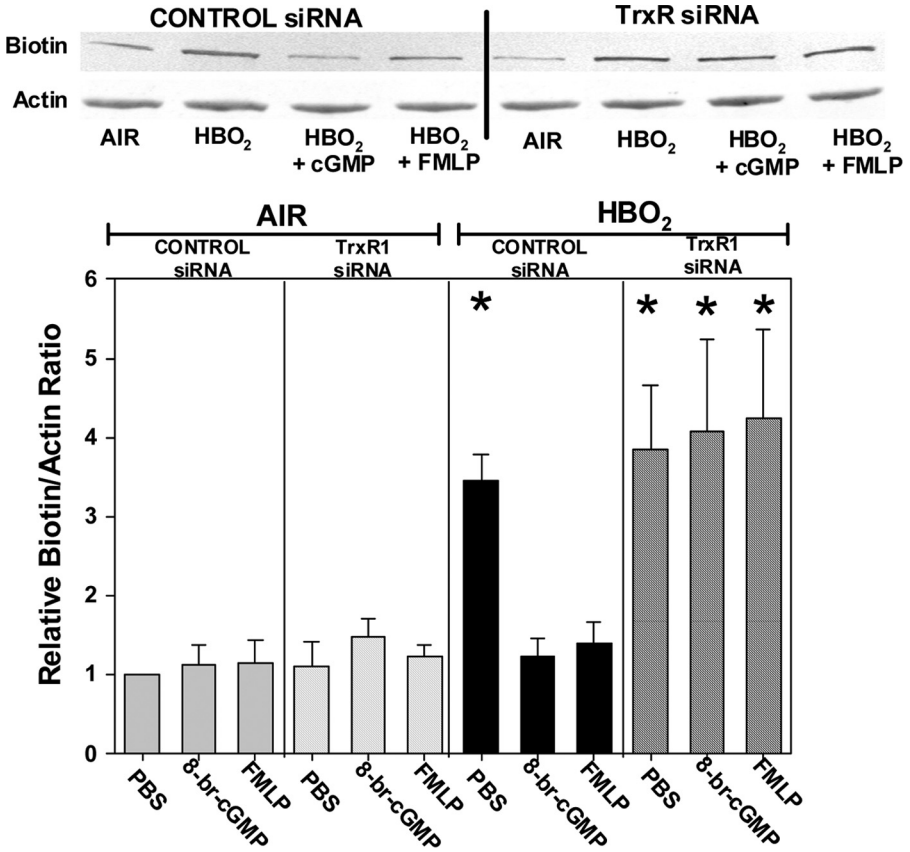

FIGURE 3. ***S*-Nitrosylated β-actin in neutrophil lysates after siRNA treatments.** Neutrophil suspensions exposed to air or 45 min at 2.0 ATA O_2 were incubated for 20 h with control, scrambled sequence siRNA or siRNA to TrxR1. Samples were centrifuged and resuspended in PBS or PBS containing 100 μM 8-Br-cGMP or 100 nM fMLP. After incubation for 10 min, cells were centrifuged, resuspended in HEN buffer, and processed for the biotin switch assay as described under "Experimental Procedures." After Western blotting, the densities of biotin-labeled and actin bands were measured, and -fold increase in biotin/actin density for each sample was compared with that measured for air-exposed cells incubated with control siRNA and then PBS that was run on the same Western blot. Data are mean ± S.E. (*error bars*) -fold increase in ratios of band densities for 4–10 independent samples; *, $p < 0.05$ (ANOVA). The blots shown at the *top* are from a representative single experiment.

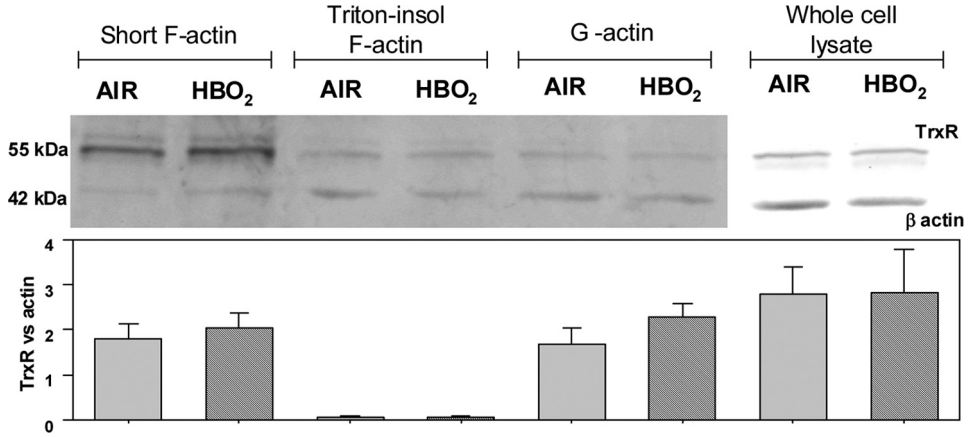

FIGURE 4. **TrxR content in neutrophil actin fractions.** Neutrophil suspensions were exposed to air (control) or 2.0 ATA O_2 for 45 min, directly placed into SDS buffer (whole cell lysate), or lysed and separated into Triton-soluble G-actin and sF-actin and Triton-insoluble actin. Western blots were probed for TrxR and β-actin. The figure shows a representative Western blot, and the *chart* depicts TrxR/actin ratios as mean ± S.E. (*error bars*) ($n = 8$ individual samplings). There are no significant differences between air-exposed (control) and HBO_2-exposed cell preparations.

trophil lysates immunoprecipitated using antibodies to TrxR, and protein bands were imaged by Coomassie staining (Fig. 5). In both control and HBO_2-exposed samples, several cytoskeletal and chaperone proteins as well as FAK were identified in the bands based on peptide MS/MS spectra as described under "Experimental Procedures."

Quantitative evaluations of immunoprecipitated proteins were conducted on G and sF-actin fractions of air and HBO_2-exposed samples. Using antibodies to TrxR, the amount of actin relative to the TrxR band density on Western blots of short F-actin fractions is shown in Fig. 6*A*. Less actin was brought down along with TrxR in HBO_2-exposed cells, and this effect

TABLE 3

TrxR activity in neutrophil lysates

TrxR activity was measured in cell lysates of air-exposed (control) or HBO_2-exposed neutrophils incubated for 10 min with just PBS or with PBS plus 100 μM 8-Br-cGMP, 100 nM FMLP, 2 μM cytochalasin D, or 1 μM latrunculin B or when cells were exposed for 5 min to UV light before lysis. The last two rows show activity when cells were lysed with Triton and processed as described under "Experimental Procedures" to obtain G-actin and sF-actin fractions rather than using whole cell lysates. TrxR activity was measured as described under "Experimental Procedures" and expressed as μmol of TNB formed/min $\times 10^2$ in 7.5 μg of neutrophil cytosol protein ($n = 7$–21). Values are mean ± S.E.

Inhibitor/Modification	Air	HBO_2
	$\mu mol/min \times 10^2$	$\mu mol/min \times 10^2$
PBS (control)	1.88 ± 0.22 (21)	8.07 ± 0.67 (21)[a]
PBS + 8-Br-cGMP	2.49 ± 0.38 (16)	2.71 ± 0.35 (16)
PBS + fMLP	2.43 ± 0.60 (16)	2.35 ± 0.64 (16)
PBS + cytochalasin D	1.50 ± 0.44 (4)	1.86 ± 0.69 (4)
PBS + latrunculin B	1.06 ± 0.35 (4)	1.20 ± 0.39 (4)
5 min UV	0.91 ± 0.18 (9)	1.03 ± 0.21 (9)
G-actin fraction	0.91 ± 0.14 (6)	6.30 ± 0.86 (6)[a]
Soluble F-actin fraction	0.87 ± 0.13 (6)	3.81 ± 0.50 (6)[a]

[a] $p < 0.05$, ANOVA.

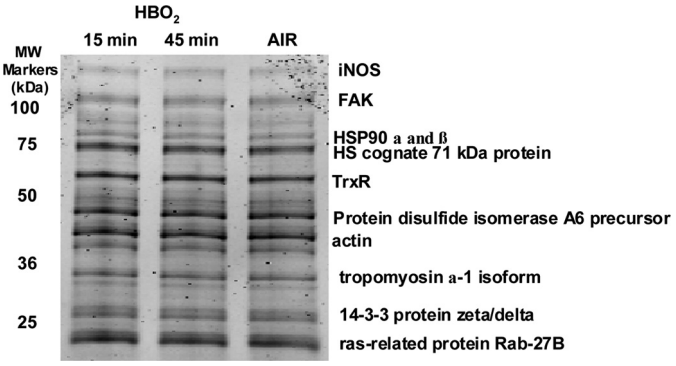

FIGURE 5. **TrxR immunoprecipitation Coomassie-stained gel.** The figure shows the band pattern for lysates of air-exposed, control, and HBO_2-exposed neutrophil lysates immunoprecipitated using anti-TrxR. Proteins listed were identified by MS/MS spectra. For nitric-oxide synthase-2 (*iNOS*) 36 peptides were identified spanning 32% of the protein; for FAK, 12 peptides were identified spanning 9% of the protein; for heat shock protein-90α (*HSP90* α), 20 peptides were identified spanning 24% of the protein; for heat shock protein-90β (*HSP90* β), 22 peptides were identified spanning 34% of the protein; for heat shock cognate 71-kDa protein, 19 peptides were identified spanning 29% of the protein; for TrxR, 10 peptides were identified spanning 18% of the protein; for protein-disulfide isomerase A6 precursor, seven peptides were identified spanning 18% of the protein; for actin, 26 peptides were identified spanning 49% of the protein; for tropomyosin α-1 isoform, seven peptides were identified spanning 26% of the protein; for 14-3-3 protein ζ/δ, 12 peptides were identified spanning 44% of the protein; for Ras-related protein Rab-27B, seven peptides were identified spanning 42% of the protein.

was reversed by fMLP or 8-Br-cGMP incubation. Particular interest in FAK was prompted because FAK is recognized to act in conjunction with a number of actin-binding proteins to bundle them with actin filaments, as summarized in the Introduction. The immunoprecipitation pattern of FAK using antibodies to TrxR was similar to that seen for actin (Fig. 6*B*). Moreover, when using antibodies to FAK, HBO_2 exposure caused a reduction of actin co-precipitation, which was also reversed by fMLP and 8-Br-cGMP (Fig. 6*C*). There was, however, no significant difference in TrxR co-precipitated with antibodies to FAK in air- or HBO_2-exposed samples. Lysates from HBO_2-exposed cells exhibited a TrxR/FAK ratio that was 0.94 ± 0.06-fold (NS, $n = 6$) that of air-exposed control cells. We did not find significant differences in co-precipitated proteins when G-actin fractions were used *versus* the sF-actin fractions (data not shown).

Time Course for Events—Results led to the question of when HBO_2-mediated events occurred during hyperoxia. Fig. 2 shows that the magnitude of SNO-actin formation was insignificantly different whether cells were exposed to HBO_2 for 15 or 45 min. Exposure to hyperoxia for just 10 min was similar and was within 2 ± 1% ($n = 3$–4 at each time point, NS) of the value found in samples after 15 min of HBO_2 (*i.e.* there was no significant difference in SNO-actin elevation following HBO_2 exposures of 10, 15, or 45 min). Fig. 7 shows that even after just 10 min of exposure to hyperoxia, β_2 integrin adherence was decreased by 50%, with complete inhibition occurring at ~45 min.

HBO_2 hastens free barbed end (FBE) formation and actin turnover (27). Compared with the rate of control, air-exposed cells, exposure to HBO_2 for 15 min increased FBE formation 2.6 ± 0.4-fold ($n = 6$, $p < 0.05$ *versus* control), whereas 45-min exposure increased FBE formation 3.9 ± 0.7-fold ($n = 21$, $p < 0.05$ *versus* control). Immunoprecipitation studies performed using FAK antibodies with lysates of cells exposed to HBO_2 for 10 min identified an increase in the actin/FAK ratio (1.47 ± 0.18-fold greater than air-exposed, control cells; $n = 4$; $p < 0.05$). No significant differences compared with control were found, however, with co-precipitation of actin or FAK using TrxR antibodies. For example, when normalized to the control cell ratios, the amount of actin co-precipitated was 0.89 ± 0.07 ($n = 5$), and FAK co-precipitated using TrxR antibodies was 0.96 ± 0.08 ($n = 5$).

Protein Co-localization Assessed by Confocal Microscopy—Immunoprecipitation studies could not be done with the Triton-insoluble F-actin. Therefore, in order to examine possible protein associations with total F-actin, we next carried out a series of imaging studies. Isolated neutrophils exposed to air (control) or 2.0 ATA O_2 for 15 or 45 min were stained with antibody to TrxR1 and with FITC-conjugated phalloidin to identify F-actin. Fig. 8 shows images as well as co-localization quantified by fluorescence in dual-stained cells. Fluorescence associated with co-localized proteins in HBO_2-exposed cells was significantly different from control at both time points, higher than control at 15 min and lower at 45 min ($p < 0.05$, two-way ANOVA). Moreover, incubation with fMLP or 8-Br-cGMP reversed alterations in co-localization due to HBO_2.

The relationship between FAK and F-actin was also examined because of observations following the immunoprecipitation studies described above. As indicated in Fig. 8, the pattern of associations of F-actin with FAK was similar to that with TrxR. Moreover, co-localization between TrxR and FAK followed a similar pattern and was the same or somewhat lower than control after fMLP or 8-Br-cGMP treatment.

TrxR and Actin Filament Vulnerability to S-Nitrosylation—Studies were done to directly assess whether TrxR could protect actin from nitrosative stress. The sF-actin fraction was isolated from neutrophils and then incubated with 200 μM SNAP. SNO-actin was quantified and expressed as the ratio of band density in the absence *versus* presence of auranofin to inhibit TrxR activity. The *first bar* in Fig. 9 demonstrates that TrxR activity inhibited SNO-actin formation by ~70%. The *second bar* demonstrates that SNO-actin formation was significantly higher if sF-actin was used from cells that had been incubated

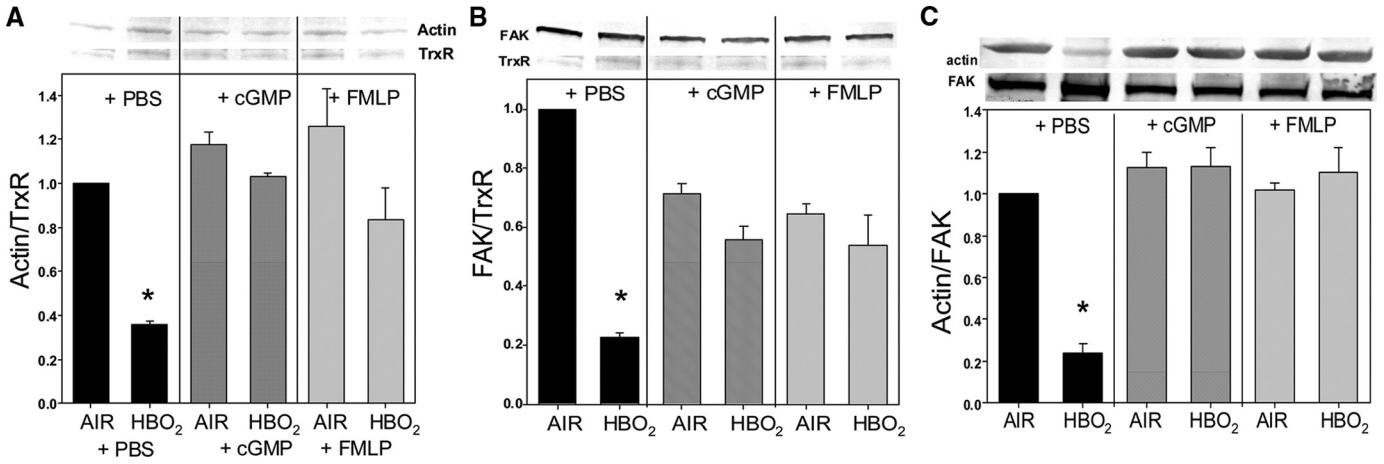

FIGURE 6. **FAK-TrxR (*A*), actin-TrxR (*B*), and actin-FAK (*C*) linkage in sF-actin fractions assessed by immunoprecipitation.** Neutrophils exposed to air (control) or 2.0 ATA O_2 for 45 min were divided and incubated for 10 min with PBS or PBS plus agonists to achieve a final concentration of 100 μM 8-Br-cGMP or 100 nM fMLP. Cells were lysed, and the sF-actin fraction was isolated and subjected to immunoprecipitation using antibodies to TrxR1 or FAK. Western blots at the *top* show typical results, and data were expressed as the ratio of β-actin (42 kDa) (*A*) or FAK (110 kDa) (*B*) band density *versus* TrxR (55 kDa) band density normalized to the ratio of the air-exposed PBS-incubated cell lysate in each sample. The ratio of actin to FAK when using antibodies to FAK is shown in *C*. Values are mean ± S.E. (*error bars*) for six independent trials; *, $p < 0.05$, ANOVA.

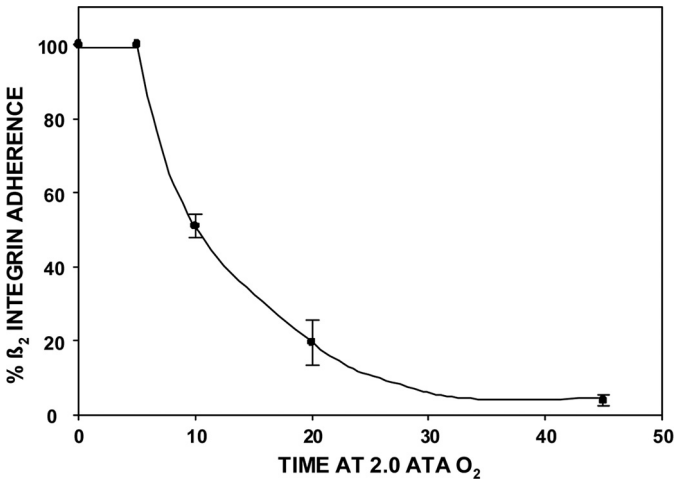

FIGURE 7. **Neutrophil adherence after exposures to hyperoxia up to 45 min.** Cells were exposed to 2.0 ATA O_2 for 5–45 min, and adherence to fibrinogen-coated plates was quantified. Values are mean ± S.E. (*error bars*); n = 3–7; *, $p < 0.05$, ANOVA.

with siRNA to TrxR1 to decrease TrxR content. As shown in the *third bar*, we also examined TrxR protection from SNAP using actin obtained from cells incubated with siRNA to FAK. Depleting cells of FAK caused a similar effect as depleting cells of TrxR.

TrxR Linkage to FAK ex Vivo—The immunoprecipitation data suggest that TrxR and FAK form a linkage within the neutrophil. Moreover, the effect of PF 573228 (Table 2) suggests that the interaction may involve the FAK kinase domain. To further examine this possibility, His-tagged kinase domain of human FAK (amino acids 393–698) was incubated with purified TrxR. Cobalt resin pull-down of His-FAK co-precipitated TrxR, and this was inhibited by PF 573228 (Fig. 10). Incubation with 5 μM PF 573228 inhibited TrxR binding/pull-down without altering FAK recovery. When using 10 μM PF 573228, the FAK detected on Western blots was reduced by 20 ± 5% (n = 3), suggesting that the inhibitor may alter protein folding and partially shield the histidine affinity tag.

Finally, we examined the effect of purified His-FAK on TrxR activity as described under "Experimental Procedures." Suspensions of TrxR exhibited an activity of 381 ± 16 ($n = 5$) units, and inclusion of FAK decreased activity by ~75% to only 95 ± 17 units ($n = 5, p < 0.05$). If 5 μM PF 573228 was included in the suspension to inhibit the FAK interaction, however, TrxR enzymatic activity was 363 ± 22 (n = 5, NS).

DISCUSSION

The goal for this investigation was to identify the mechanism for reversal of SNO-actin in HBO_2-exposed neutrophils. We conclude from the adherence and biotin switch studies in cells preincubated with siRNA species that TrxR is required for actin denitrosylation when HBO_2-exposed neutrophils are incubated with fMLP or 8-Br-cGMP (Figs. 1–3). The role for TrxR in decreasing SNO-actin is also supported by effects of the chemical inhibitors, 1-chloro-2,4-dinitrobenzene and auranofin (Table 1).

We have reported that fMLP and 8-Br-cGMP will slow actin turnover in HBO_2-exposed cells (27). Our finding that cytochalasin treatment will abrogate the HBO_2-mediated elevation of SNO-actin is consistent with these previous reports and indicates that actin turnover with increased FBE formation establishes the imbalance that impedes TrxR from causing SNO-actin removal. It is clear, however, that the process is more complicated than merely involving TrxR. The majority of cellular TrxR is in the cytoplasm, and partitioning to various cell fractions based on Triton solubility was not significantly altered by HBO_2 (Fig. 4). Demonstrating that TrxR activity was increased, not decreased, after hyperoxia posed a paradox that now appears related to enzyme linkage to FAK (Table 3).

MS/MS evaluation of protein bands identified after TrxR immunoprecipitation led to an interest in FAK (Fig. 5). The apparent association between TrxR and several other proteins will require more rigorous study for verification. It is perhaps not surprising that associations with a number of cytoskeletal proteins other than actin may occur. Possible associations with proteins such as heat shock protein 90 and heat shock cognate

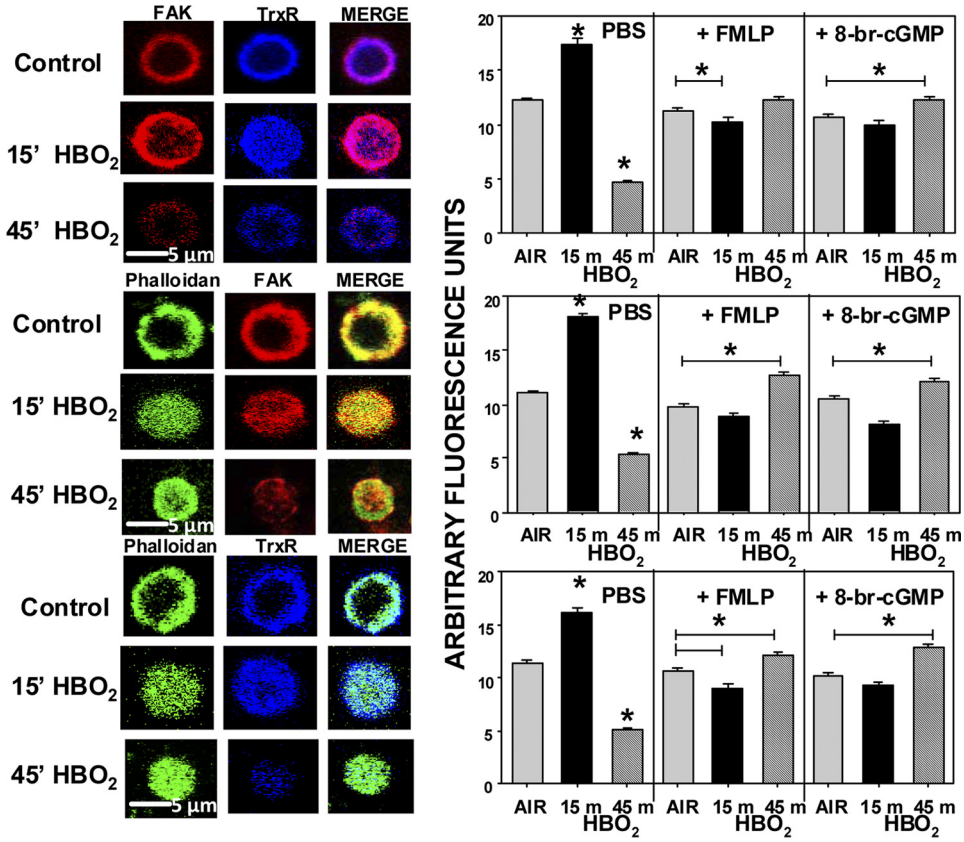

FIGURE 8. **Protein co-localizations with F-actin in neutrophil images.** Neutrophils exposed to air or HBO_2 *ex vivo* were placed on fibrinogen-coated slides, permeabilized and stained as described under "Experimental Procedures." *Bar graphs* show merged fluorescence intensity, which reflects protein co-localizations. These data were obtained with cells from mice in 3–7 independent experiments by analyzing 30–65 neutrophils in each trial. Values in *bar graphs* are mean ± S.E. (*error bars*); *, $p < 0.001$ *versus* air-exposed cells.

71 kDa protein are consistent with their roles as chaperones. Activation of all three nitric-oxide synthase isoforms occurs upon association with actin filaments, and the possible link with inducible nitric-oxide synthase will also require further study (54, 55).

Immunoprecipitation experiments showed that HBO_2 exposure for 45 min decreased the association between FAK and TrxR in the sF-actin fraction by about 80% (Fig. 6). Reversal of this situation by fMLP and 8-Br-cGMP, along with the HBO_2-mediated diminished associations between actin and TrxR and between FAK and actin, provides insight into how these agonists abrogate HBO_2 effects. Confocal microscopy findings support the immunoprecipitation results and add further information. Results clearly show not only the diminished interactions among TrxR, FAK, and F-actin after 45 min but also increased associations with just 15-min exposure to hyperoxia. Immunoprecipitation studies at 15 min identified an elevation in FAK linkage to actin, but studies using TrxR antibodies did not identify changes from control in FAK-to-TrxR or actin-to-TrxR pull-down in the sF-actin fraction. This may be due in part to greater HBO_2-mediated perturbations for cytoskeletal Triton-insoluble actin filaments that cannot be discerned with immunoprecipitation. Alternatively, it is possible that the conditions established for the immunoprecipitation studies cause the proteins to disengage.

The time course studies indicate that there is a lag between SNO-actin formation (Fig. 2), increased FBEs, and impaired β_2 integrin function (Fig. 7). SNO-actin is near maximum within 10 min of exposure to hyperoxia, FBE formation increases progressively with time, and maximum β_2 integrin inhibition does not occur until cells have been exposed for ~45 min. Taken in association with our previous studies, neutrophil β_2 integrin inhibition by HBO_2 can be divided into several steps (26, 27). 1) SNO-actin is formed when reactive species are generated by inducible nitric-oxide synthase and myeloperoxidase. 2) VASP exhibits enhanced affinity for *S*-nitrosylated sF-actin. 3) This increases actin FBE formation because of subsequent recruitment by VASP of cyclic AMP-dependent and cyclic GMP-dependent protein kinase, which, in turn, mediate Rac 1 and 2 activation. 4) Actin FBE turnover becomes progressively more rapid with HBO_2 exposures up to ~45 min and inhibits β_2 integrin clustering and thus β_2 integrin adhesion. Additional events based on current studies include the following. 5) The increased actin turnover rate eventually causes FAK to dissociate from sF-actin (determination of whether increased FAK linkage to F-actin at 10–15 min hyperoxia is due to actin turnover or some other process will require further work). 6) TrxR normally linked to FAK in the sF-actin fraction and thus in proximity to SNO-actin can mediate denitrosylation. 7) However, when FAK dissociates, the TrxR no longer remains linked to FAK. 8) In this way, although cytosolic TrxR activity is elevated, the enzyme cannot affect denitrosylation.

The *ex vivo* studies with SNAP support the cell fraction studies and indicate that TrxR provides actin protection from oxi-

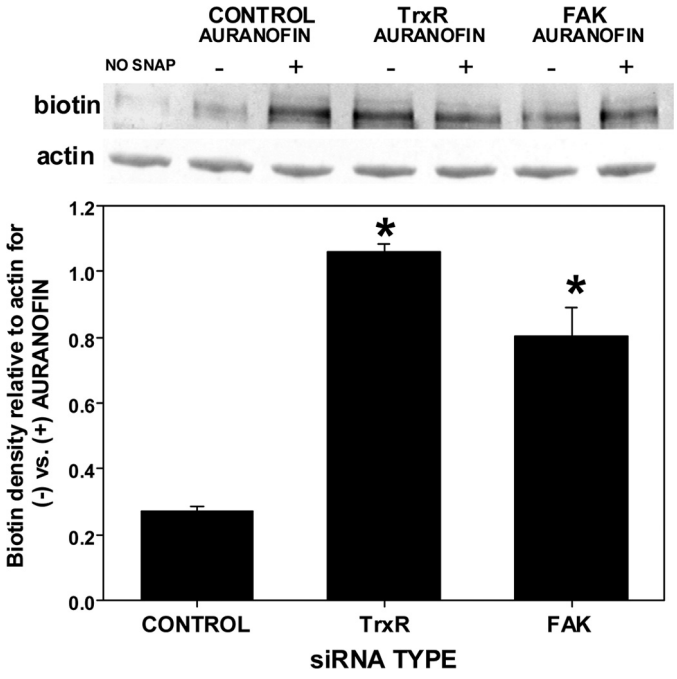

FIGURE 9. **TrxR protects actin from *S*-nitrosylation.** Neutrophils were isolated and incubated for 20 h with control siRNA or siRNA to TrxR or FAK. Cells were lysed, the sF-actin fraction was isolated and divided into two, and 1 μM auranofin was added to one sample. Both samples were incubated with 200 μM SNAP for 1 h at room temperature, and then *S*-nitrosylation was assessed by the biotin switch assay. The Western blot at the *top* demonstrates typical experimental results, and data are expressed as the difference in density of the biotin/actin band ratio of samples incubated in the absence *versus* presence of auranofin, a TrxR inhibitor. Therefore, values closer to 1.0 demonstrate inability of TrxR in the sample to protect against *S*-nitrosylation. Values are mean ± S.E. (*error bars*) for four experiments; *, $p < 0.05$, ANOVA.

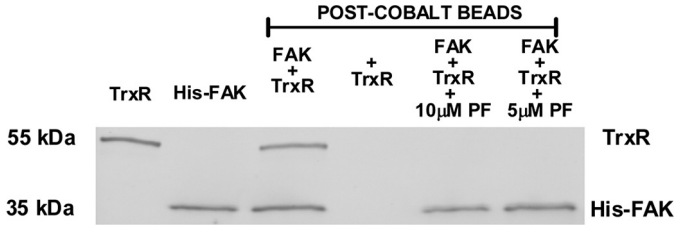

FIGURE 10. **TrxR-FAK *ex vivo* attachment with isolated enzymes.** Purified TrxR was incubated with a His-tagged kinase domain fragment of human FAK as described under "Experimental Procedures." Where indicated, 5 or 10 μM PF 573228 was added to FAK suspensions 10 min before the addition of TrxR. After 1-h incubations, protein suspensions were passed through cobalt resin, and the bound protein was eluted and then subjected to Western blotting. The pattern shown in the figure was identical in four replicate trials. The *first two lanes* show blots using only the single protein solutions (TrxR or His-FAK), whereas *lanes 3–6* show proteins eluted from cobalt resin. *Lane 3* shows His-FAK plus TrxR, and *lane 4* shows the result when the TrxR solution is incubated with resin (*e.g.* no TrxR binds to resin). The *last two lanes* show results when 5 or 10 μM PF 573228 was added to His-FAK plus TrxR solutions. No TrxR was detected in these suspensions, and at 10 μM PF 573228, the FAK band density was 20 ± 5% (S.E.; $n = 3$) lower than with no inhibitor or just 5 μM PF 573228.

dative stress. Further, FAK is required for TrxR-mediated protection (Fig. 9). Results also demonstrate that TrxR activity is constrained by linkage to FAK. This is most clearly shown with studies of purified TrxR and His-FAK. Given that immunoprecipitation studies show less FAK linked to TrxR in sF-actin from cells exposed to HBO_2 45 min, the *ex vivo* studies provide an explanation for the elevation of TrxR activity in the cytosol after HBO_2 exposure.

Results show that slowing actin turnover will allow FAK to reassociate with sF-actin; TrxR then links to FAK, which drives SNO-actin removal and restores β_2 integrin function. These new findings increase understanding of TrxR activity, but other antioxidant enzymes, such as *S*-nitrosoglutathione reductase and glutathione reductase, could also be involved with neutrophil protein denitrosylation. Cell contents of these enzymes were only partially reduced with siRNA treatments. Moreover, if HBO_2-exposed cells are incubated with lipoic acid, actin denitrosylation occurs, and TrxR depletion alone does not inhibit this response.

FAK functions predominantly as a scaffolding protein. Because we found that a FAK kinase domain inhibitor (PF 573228) achieved the same effect as depleting cells of FAK using siRNA, we sought direct evidence that the FAK kinase domain plays a role with TrxR interactions. Based on the His-FAK pull-down studies, TrxR associates in this region, and PF 573228, which acts at the ATP-binding site (53), inhibits the interaction (Fig. 10). The only other protein known to interact with FAK within its kinase domain is FAK family-interacting protein of 200 kDa (FIP200), which inhibits FAK activity (56). A comparison of amino acid sequences between human TrxR and FIP200 using the NCBI basic local alignment search tool (BLAST) had a maximum score of just 16.9 and *E* value of 6.3. Hence, the proteins exhibit little similarity. TrxR contains a caveolin-binding motif (amino acids 454–463) and binds to caveolin-1, an interaction that inhibits TrxR activity (57). FAK does not contain a caveolin scaffolding domain. Obviously, the characteristics of TrxR-FAK binding will require additional study.

The simple conditions established for the *ex vivo* His-FAK pull-down experiments suggest that FAK kinase activity is not required for TrxR binding or to inhibit TrxR activity. Most intracellular FAK kinase activity is actually performed by Src family kinases that associate following phosphorylation of FAK tyrosine 397 (46). The purified FAK fragment used in our studies was expressed in baculovirus-infected Sf9 cells. We are aware that spurious hyperphosphorylation adjacent to histidine affinity tags can complicate studies using high level recombinant protein kinases (58). Although we cannot rule out an involvement of such complications, we think that they are unlikely given the results with intact neutrophils. FAK functions are facilitated by physical forces as FAK is recruited to the juxtamembrane space to form focal adhesions, the proximal step to cell adherence (59). This includes homo-oligomer formation that is initiated by enzyme clustering at focal contacts followed by tyrosine 397 autophosphorylation that triggers kinase activity (60). The point with our work is that the FAK-TrxR interaction is apparent with non-adherent neutrophils and also monomeric His-FAK, conditions where FAK phosphorylation/kinase activity is unlikely to occur.

These results demonstrate that TrxR plays a role in cytoskeletal control in neutrophils. There is precedence for this in other cell types. TrxR overexpression inhibits protein kinase C-mediated HEK-293 cell motility (61). A splice variant of TrxR1 in human Leydig cells induces cytoplasmic filaments and cell membrane filopodia. The mechanism remains obscure because the protein exhibits only partial co-localization with actin and may act as a novel actin nucleation center (62, 63). Moreover,

there is a physical interaction between thioredoxin and actin that assists with stabilizing the cytoskeleton of SH-SYS5Y cells (64).

In conclusion, this project advances understanding of cytoskeletal control in neutrophils and regulation of β_2 integrin function. Its immediate clinical relevance is to provide a biochemical explanation for how HBO_2 can impede β_2 integrin adherence and thus ameliorate insults, such as reperfusion injuries, yet treatment does not render the host immunocompromised. The risk/benefit ratio of HBO_2 appears favorable under most conditions. These results provide further assurance as to its safety and may prompt greater investigation of its clinical efficacy. Questions persist regarding the nature of the TrxR-FAK chemical interaction and whether it has functional impact on adhesion and cytoskeletal control beyond its apparent antioxidant role for actin denitrosylation.

Acknowledgments—Mass spectrometry analysis was provided by the Proteomics Core Facility, University of Pennsylvania, supported by National Institutes of Health Grants P30CA016520 (to the Abramson Cancer Center) and ES013508-04 (to the Center of Excellence in Environmental Toxicology).

REFERENCES

1. Brown, E. J., and Lindberg, F. P. (1996) Leukocyte adhesion molecules in host defence against infection. *Ann. Med.* **28,** 201–208
2. Thom, S. R. (1993) Functional inhibition of leukocyte B2 integrins by hyperbaric oxygen in carbon monoxide-mediated brain injury in rats. *Toxicol. Appl. Pharmacol.* **123,** 248–256
3. Thom, S. R., Mendiguren, I., Hardy, K., Bolotin, T., Fisher, D., Nebolon, M., and Kilpatrick, L. (1997) Inhibition of human neutrophil β2-integrin-dependent adherence by hyperbaric O_2. *Am. J. Physiol.* **272,** C770–C777
4. Kalns, J., Lane, J., Delgado, A., Scruggs, J., Ayala, E., Gutierrez, E., Warren, D., Niemeyer, D., George Wolf, E., and Bowden, R. A. (2002) Hyperbaric oxygen exposure temporarily reduces Mac-1-mediated functions of human neutrophils. *Immunol. Lett.* **83,** 125–131
5. Labrouche, S., Javorschi, S., Leroy, D., Gbikpi-Benissan, G., and Freyburger, G. (1999) Influence of hyperbaric oxygen on leukocyte functions and hemostasis in normal volunteer divers. *Thromb. Res.* **96,** 309–315
6. Zamboni, W. A., Roth, A. C., Russell, R. C., Graham, B., Suchy, H., and Kucan, J. O. (1993) Morphologic analysis of the microcirculation during reperfusion of ischemic skeletal muscle and the effect of hyperbaric oxygen. *Plast. Reconstr. Surg.* **91,** 1110–1123
7. Martin, J. D., and Thom, S. R. (2002) Vascular leukocyte sequestration in decompression sickness and prophylactic hyperbaric oxygen therapy in rats. *Aviat. Space Environ. Med.* **73,** 565–569
8. Atochin, D. N., Fisher, D., Demchenko, I. T., and Thom, S. R. (2000) Neutrophil sequestration and the effect of hyperbaric oxygen in a rat model of temporary middle cerebral artery occlusion. *Undersea Hyperb. Med.* **27,** 185–190
9. Tähepõld, P., Vaage, J., Starkopf, J., and Valen, G. (2003) Hyperoxia elicits myocardial protection through a nuclear factor κB-dependent mechanism in the rat heart. *J. Thorac. Cardiovasc Surg.* **125,** 650–660
10. Tähepold, P., Valen, G., Starkopf, J., Kairane, C., Zilmer, M., and Vaage, J. (2001) Pretreating rats with hyperoxia attenuates inschemia-reperfusion injury of the heart. *Life Sci.* **68,** 1629–1640
11. Ueno, S., Tanabe, G., Kihara, K., Aoki, D., Arikawa, K., Dogomori, H., and Aikou, T. (1999) Early postoperative hyperbaric oxygen therapy modifies neutrophile activation. *Hepatol. Gastroenterology* **46,** 1798–1799
12. Wong, H. P., Zamboni, W. A., and Stephenson, L. L. (1996) Effect of hyperbaric oxygen on skeletal muscle necrosis following primary and secondary ischemia in a rat model. *Surg. Forum* 705–707
13. Yang, Z. J., Bosco, G., Montante, A., Ou, X. I., and Camporesi, E. M. (2001) Hyperbaric O_2 reduces intestinal ischemia-reperfusion-induced TNF-α production and lung neutrophil sequestration. *Eur. J. Appl. Physiol.* **85,** 96–103
14. Sharifi, M., Fares, W., Abdel-Karim, I., Koch, J. M., Sopko, J., Adler, D., and the Hyperbaric Oxygen Therapy in Percutaneous Coronary Interventions Investigators (2004) Usefulness of hyperbaric oxygen therapy to inhibit restenosis after percutaneous coronary intervention for acute myocardial infarction or unstable angina pectoris. *Am. J. Cardiol.* **93,** 1533–1535
15. Sharifi, M., Fares, W., Abdel-Karim, I., Petrea, D., Koch, J. M., Adler, D., Sopko, J., and the Hyperbaric Oxygen Therapy in Percutaneous Coronary Interventions (HOT-PI) Investigators (2002) Inhibition of restenosis by hyperbaric oxygen. A novel indication for an old modality. *Cardiovasc. Radiat. Med.* **3,** 124–126
16. Shandling, A. H., Ellestad, M. H., Hart, G. B., Crump, R., Marlow, D., Van Natta, B., Messenger, J. C., Strauss, M., and Stavitsky, Y. (1997) Hyperbaric oxygen and thrombolysis in myocardial infarction. The HOT MI pilot study. *Am. Heart J.* **134,** 544–550
17. Stavitsky, Y., Shandling, A. H., Ellestad, M. H., Hart, G. B., Van Natta, B., Messenger, J. C., Strauss, M., Dekleva, M. N., Alexander, J. M., Mattice, M., and Clarke, D. (1998) Hyperbaric oxygen and thrombolysis in myocardial infarction. The "HOT MI" randomized multicenter study. *Cardiology* **90,** 131–136
18. Weaver, L. K., Hopkins, R. O., Chan, K. J., Churchill, S., Elliott, C. G., Clemmer, T. P., Orme, J. F., Jr., Thomas, F. O., and Morris, A. H. (2002) Hyperbaric oxygen for acute carbon monoxide poisoning. *N. Engl. J. Med.* **347,** 1057–1067
19. Alex, J., Laden, G., Cale, A. R., Bennett, S., Flowers, K., Madden, L., Gardiner, E., McCollum, P. T., and Griffin, S. C. (2005) Pretreatment with hyperbaric oxygen and its effect on neuropsychometric dysfunction and systemic inflammatory response after cardiopulmonary bypass. A prospective randomized double-blind trial. *J. Thorac. Cardiovasc. Surg.* **130,** 1623–1630
20. Juttner, B., Scheinichen, D., Bartsch, S., Heine, J., Ruschulte, H., Elsner, H., Franko, W., and Jaeger, K. (2003) Lack of toxic side effects in neutrophils following hyperbaric oxygen. *Undersea Hyperbar. Med.* **30,** 305–311
21. Mileski, W. J., Sikes, P., Atiles, L., Lightfoot, E., Lipsky, P., and Baxter, C. (1993) Inhibition of leukocyte adherence and susceptibility to infection. *J. Surg. Res.* **54,** 349–354
22. Mileski, W. J., Winn, R. K., Vedder, N. B., Pohlman, T. H., Harlan, J. M., and Rice, C. L. (1990) Inhibition of CD18-dependent neutrophil adherence reduces organ injury after hemorrhagic shock in primates. *Surgery* **108,** 206–212
23. Thom, S. R., Lauermann, M. W., and Hart, G. B. (1986) Intermittent hyperbaric oxygen therapy for reduction of mortality in experimental polymicrobial sepsis. *J. Infect. Dis.* **154,** 504–510
24. Ross, R. M., and McAllister, T. A. (1965) Protective action of hyperbaric oxygen in mice with pneumococcal septicemia *Lancet* **1,** 579–581
25. Buras, J., Holt, D., Orlow, D., Belikoff, B., Pavlides, S., and Reenstra, W. (2006) Hyperbaric oxygen protects from sepsis mortality via an interleukin-10-dependent mechanism. *Crit. Care Med.* **34,** 2624–2629
26. Thom, S. R., Bhopale, V. M., Mancini, D. J., and Milovanova, T. N. (2008) Actin *S*-nitrosylation inhibits neutrophil β-2 integrin function. *J. Biol. Chem.* **283,** 10822–10834
27. Thom, S. R., Bhopale, V. M., Yang, M., Bogush, M., Huang, S., and Milovanova, T. (2011) Neutrophil β2 integrin inhibition by enhanced interactions of vasodilator stimulated phosphoprotein with *S*-nitrosylated actin. *J. Biol. Chem.* **286,** 32854–32865
28. Thom, S. R. (2009) Oxidative stress is fundamental to hyperbaric oxygen therapy. *J. Appl. Physiol.* **106,** 988–995
29. Marasco, W. A., Phan, S. H., Krutzsch, H., Showell, H. J., Feltner, D. E., Nairn, R., Becker, E. L., and Ward, P. A. (1984) Purification and identification of formyl-methionyl-leucyl-phenylalanine as the major peptide neutrophil chemotactic factor produced by *Escherichia coli*. *J. Biol. Chem.* **259,** 5430–5439
30. Stoyanovsky, D. A., Tyurina, Y. Y., Tyurin, V. A., Anand, D., Mandavia, D. N., Gius, D., Ivanova, J., Pitt, B., Billiar, T. R., and Kagan, V. E. (2005) Thioredoxin and lipoic acid catalyze the denitrosation of low molecular weight and protein *S*-nitrosothiols. *J. Am. Chem. Soc.* **127,** 15815–15823

31. Matuda, S., and Saheki, T. (1982) Intracellular distribution and biosynthesis of lipoamide dehydrogenase in rat liver. *J. Biochem.* **91,** 553–561
32. Sun, Q. A., Su, D., Novoselov, S. V., Carlson, B. A., Hatfield, D. L., and Gladyshev, V. N. (2005) Reaction mechanism and regulation of mammalian thioredoxin/glutathione reductase. *Biochemistry* **44,** 14528–14537
33. Sun, Q. A., Kirnarsky, L., Sherman, S., and Gladyshev, V. N. (2001) Selenoprotein oxidoreductase with specificity for thioredoxin and glutathione systems. *Proc. Natl. Acad. Sci. U.S.A.* **98,** 3673–3678
34. Arnér, E. S., and Holmgren, A. (2000) Physiological functions of thioredoxin and thioredoxin reductase. *Eur. J. Biochem.* **267,** 6102–6109
35. Rigobello, M. P., Callegaro, M. T., Barzon, E., Benetti, M., and Bindoli, A. (1998) Purification of mitochondrial thioredoxin reductase and its involvement in the redox regulation of membrane permeability. *Free Radic. Biol. Med.* **24,** 370–376
36. Benhar, M., Forrester, M. T., and Stamler, J. S. (2009) Protein denitrosylation. Enzymatic mechanisms and cellular functions. *Nat. Rev. Mol. Cell Biol.* **10**
37. Foster, M. W., Liu, L., Zeng, M., Hess, D. T., and Stamler, J. S. (2009) A genetic analysis of nitrosative stress. *Biochemistry* **48,** 792–799
38. Schlaepfer, D. D., Mitra, S. K., and Ilic, D. (2004) Control of motile and invasive cell phenotypes by focal adhesion kinase. *Biochim. Biophys. Acta* **1692,** 77–102
39. Tabassam, F. H., Umehara, H., Huang, J. Y., Gouda, S., Kono, T., Okazaki, T., van Seventer, J. M., and Domae, N. (1999) β2-integrin, LFA-1, and TCR/CD3 synergistically induce tyrosine phosphorylation of focal adhesion kinase ($pp125^{FAK}$) in PHA-activated T cells. *Cell Immunol.* **193,** 179–184
40. Sada, K., Minami, Y., and Yamamura, H. (1997) Relocation of Syk protein-tyrosine kinase to the actin filament network and subsequent association with Fak. *Eur. J. Biochem.* **248,** 827–833
41. Totani, L., Piccoli, A., Manarini, S., Federico, L., Pecce, R., Martelli, N., Cerletti, C., Piccardoni, P., Lowell, C. A., Smyth, S. S., Berton, G., and Evangelista, V. (2006) Src-family kinases mediate an outside-in signal necessary for B2 integrins to achieve full activation and sustain firm adhesion of polymorphonuclear leukocytes tethered on E-selectin. *Biochem. J.* **396,** 89–98
42. Serrels, B., Serrels, A., Brunton, V. G., Holt, M., McLean, G. W., Gray, C. H., Jones, G. E., and Frame, M. C. (2007) Focal adhesion kinase controls actin assembly via a FERM-mediated interaction with the Arp2/3 complex. *Nat. Cell Biol.* **9,** 1046–1056
43. Ilić, D., Furuta, Y., Kanazawa, S., Takeda, N., Sobue, K., Nakatsuji, N., Nomura, S., Fujimoto, J., Okada, M., and Yamamoto, T. (1995) Reduced cell motility and enhanced focal adhesion contact formation in cells from FAK-deficient mice. *Nature* **377,** 539–544
44. Clark, E. A., and Brugge, J. S. (1995) Integrins and signal transduction pathways. The road taken. *Science* **268,** 233–239
45. García-Alvarez, B., de Pereda, J. M., Calderwood, D. A., Ulmer, T. S., Critchley, D., Campbell, I. D., Ginsberg, M. H., and Liddington, R. C. (2003) Structural determinants of integrin recognition by talin. *Mol. Cell* **11,** 49–58
46. Arold, S. T. (2011) How focal adhesion kinase achieves regulation by linking ligand binding, localization and action. *Curr. Opin. Struct. Biol.* **21,** 808–813
47. Schaller, M. D., Otey, C. A., Hildebrand, J. D., and Parsons, J. T. (1995) Focal adhesion kinase and paxillin bind to peptides mimicking β integrin cytoplasmic domains. *J. Cell Biol.* **130,** 1181–1187
48. Parsons, J. T. (2003) Focal adhesion kinase. The first ten years. *J. Cell Sci.* **116,** 1409–1416
49. Zheng, D., Kurenova, E., Ucar, D., Golubovskaya, V., Magis, A., Ostrov, D., Cance, W. G., and Hochwald, S. N. (2009) Targeting of the protein interaction site between FAK and IGF-1R. *Biochem. Biophys. Res. Commun.* **388,** 301–305
50. Wang, X., Kettenhofen, N. J., Shiva, S., Hogg, N., and Gladwin, M. T. (2008) Copper dependence of the biotin switch assay. Modified assay for measuring cellular and blood nitrosated proteins. *Free Radic. Biol. Med.* **44,** 1362–1372
51. Hill, K. E., McCollum, G. W., and Burk, R. F. (1997) Determination of thioredoxin reductase activity in rat liver supernatant. *Anal. Biochem.* **253,** 123–125
52. Thom, S. R., Bhopale, V. M., Fisher, D., Zhang, J., and Gimotty, P. (2004) Delayed neuropathology after carbon monoxide poisoning is immune-mediated. *Proc. Natl. Acad. Sci. U.S.A.* **101,** 13660–13665
53. Slack-Davis, J. K., Martin, K. H., Tilghman, R. W., Iwanicki, M., Ung, E. J., Autry, C., Luzzio, M. J., Cooper, B., Kath, J. C., Roberts, W. G., and Parsons, J. T. (2007) Cellular characterization of a novel focal adhesion kinase inhibitor. *J. Biol. Chem.* **282,** 14845–14852
54. Su, Y., Kondrikov, D., and Block, E. R. (2005) Cytoskeletal regulation of nitric-oxide synthase. *Cell Biochem. Biophys.* **43,** 439–449
55. Kone, B. C., Kuncewicz, T., Zhang, W., and Yu, Z. Y. (2003) Protein interactions with nitric oxide synthases. Controlling the right time, the right place, and the right amount of nitric oxide. *Am. J. Physiol.* **285,** F178–F190
56. Abbi, S., Ueda, H., Zheng, C., Cooper, L. A., Zhao, J., Christopher, R., and Guan, J. L. (2002) Regulation of focal adhesion kinase by a novel protein inhibitor, FIP200. *Mol. Biol. Cell* **13,** 3178–3191
57. Volonte, D., and Galbiati, F. (2009) Inhibition of thioredoxin reductase 1 by caveolin 1 promotes stress-induced premature senescence. *EMBO Rep.* **10,** 1334–1340
58. Du, P., Loulakis, P., Luo, C., Mistry, A., Simons, S. P., LeMotte, P. K., Rajamohan, F., Rafidi, K., Coleman, K. G., Geoghegan, K. F., and Xie, Z. (2005) Phosphorylation of serine residues in histidine tag sequences attached to recombinant protein kinases. A cause of heterogeneity in mass and complications in function. *Protein Expr. Purif.* **44,** 121–129
59. Kanchanawong, P., Shtengel, G., Pasapera, A. M., Ramko, E. B., Davidson, M. W., Hess, H. F., and Waterman, C. M. (2010) Nanoscale architecture of integrin-based cell adhesions. *Nature* **468,** 580–584
60. Toutant, M., Costa, A., Studler, J. M., Kadaré, G., Carnaud, M., and Girault, J. A. (2002) Alternative splicing controls the mechanisms of FAK autophosphorylation. *Mol. Cell Biol.* **22,** 7731–7743
61. Sroka, J., Antosik, A., Czyz, J., Nalvarte, I., Olsson, J. M., Spyrou, G., and Madeja, Z. (2007) Overexpression of thioredoxin reductase 1 inhibits migration of HEK-293 cells. *Biol. Cell* **99,** 677–687
62. Dammeyer, P., Damdimopoulos, A. E., Nordman, T., Jiménez, A., Miranda-Vizuete, A., and Arnér, E. S. (2008) Induction of cell membrane protrusions by the N-terminal glutaredoxin domain of a rare splice variant of human thioredoxin reductase 1. *J. Biol. Chem.* **283,** 2814–2821
63. Damdimopoulou, P. E., Miranda-Vizuete, A., Arnér, E. S., Gustafsson, J. A., and Damdimopoulos, A. E. (2009) The human thioredoxin reductase-1 splice variant TXNRD1_v3 is an atypical inducer of cytoplasmic filaments and cell membrane filopodia. *Biochim. Biophys. Acta* **1793,** 1588–1596
64. Wang, X., Ling, S., Zhao, D., Sun, Q., Li, Q., Wu, F., Nie, J., Qu, L., Wang, B., Shen, X., Bai, Y., Li, Y., and Li, Y. (2010) Redox regulation of actin by thioredoxin-1 is mediated by the interaction of the proteins via cysteine 62. *Antioxid. Redox Signal.* **13,** 565–573